Tight-binding calculation of the band structure of Silicon

Gernot Pfanner

1 Introduction

1.1 Basic approximations

A typical solid contains 10^{23} atoms and a much greater number of electrons. Therefore it is difficult (or pointless) to keep track of the motion of all particles. For this reason, solid states physics makes some basic simplifications to get information about the atomic structure of materials (as well as its electronic properties).

Firstly, one distinguishes between two kinds of electrons: "core"- and "valence"-electrons. The former includes all electrons in filled orbitals. Those electrons are mostly localized around the nuclei, and we can put them formally together with the nuclei to the so-called "ion cores". In the case of Silicon this suits for the $1s^2$-, $2s^2$-, $2p^6$-orbitals. By the latter, the valence electrons, we mean all electrons, which are in incompletely filled shells, e.g. for Silicon: the $3s$- and $3p$-shell. We will be mainly interested in these particles, since they are responsible for bonds to other atoms.

Another common assumption is the "Born-Oppenheimer"-approximation (adiabatic approximation). The nuclei are much heavier than the surrounding electrons, and hence they move much more slowly. This means practially that we just have to solve the Schrödinger equation for the electrons alone (with the nuclei contributing to the energy).

The third important simplification is the "mean-field" approximation: Each electron experiences the same average *potential V(r)*.

With these approximations we end up with the following Schrödinger equation for an electron [1]:

$$H_{1e}\Phi_n(\mathbf{r}) = (\frac{\mathbf{p}^2}{2m} + V(\mathbf{r}))\Phi_n(\mathbf{r}) = E_n\Phi_n(\mathbf{r}) \tag{1}$$

Besides this *electronic Hamiltonian* one usually has an $H_{ion}(\vec{R}_j)$ (for the ionic motion under the influence of the ionic potentials) plus an $H_{e-ion}(\vec{r}_i, \delta\vec{R}_j)$ (for the electron-phonon interaction). But this takes us off the road. At this point it is worthwile to mention, that even the alleged simple problem of equation (1) can only be solved numerically (with the real difficulty laying in the determination of $V(r)$).

1.2 Basic numerical methods

There are two basic methods for computing structures and properties of materials:

- the "ab initio" ("first principles")

- the "(semi) empirical"-methods

The former do not include any empirically or experimentally derived quantities whereas the latter do.

Ab-initio-methods are especially useful for predicting the properties of new materials and for predicting trends across a wide range of materials. Typical representatives are "Quantum Monte Carlo"- (QMC)-, "Hartree-Fock"- (HF)-, and "Density-Functional"- (DF)-methods. The particular scaling depends - among other things - on the *number of atoms* N. For guidance, QMC usually scales almost exponentially with N, whereas HF $\sim N^4$ and DF $\sim N^3$. Illustratively speaking, this means that e.g. for HF and DF, a 1000-fold increase in computer power only buys a 10-fold increase in system size. But we will not make usage of ab-initio-methods, and so I refer the interested reader to [2] and [3].

(Semi-)empirical-methods gain importance the more atoms we look at. Tight-binding (TB) belongs to these techniques. It starts in principle from ab-initio (hence an exact, self-consistent[1] Hamiltonian with appropriate approximations), but in the course of action one neglects or drops many terms in H. This relationship has been sketched in [4] (and references therein). The typical scaling of TB is $\sim N^3$.

At this point, one has to mention "linear scaling" algorithms, which (as the name implies) scales with N. Those techniques may be classified into "recursion"- and "minimization"-methods. Recursion (Momentum)-methods use a theorem (the "momentum theorem"), which relates the electronic structure of an atom to the local environment. In practical use these methods are restricted to tight-binding models. On the other hand, variational methods try to minimize the energy functional. In any case linear scaling-algorithms are not necessarily more feasible than their original counterparts. For tight-binding-methods this "crossover" point is about 100 atoms. In other words, just for systems with more than 100 atoms, linear-scaling-algorithms are more efficiently. One has to bear in mind as well, that those algorithms are an additional approximation and they all depend on the concept of locality in quantum mechanics. For further reading on this topic, I suggest [5] (as for a general overview) and Section 3 in [4] (as for the concrete appliance to tight-binding models)

2 The method

2.1 Overview

The basic idea of the tight-binding method is, that one writes the eigenstates of the Hamiltonian in an atomic-like basis set. Then one replaces the exact many-body Hamil-

---

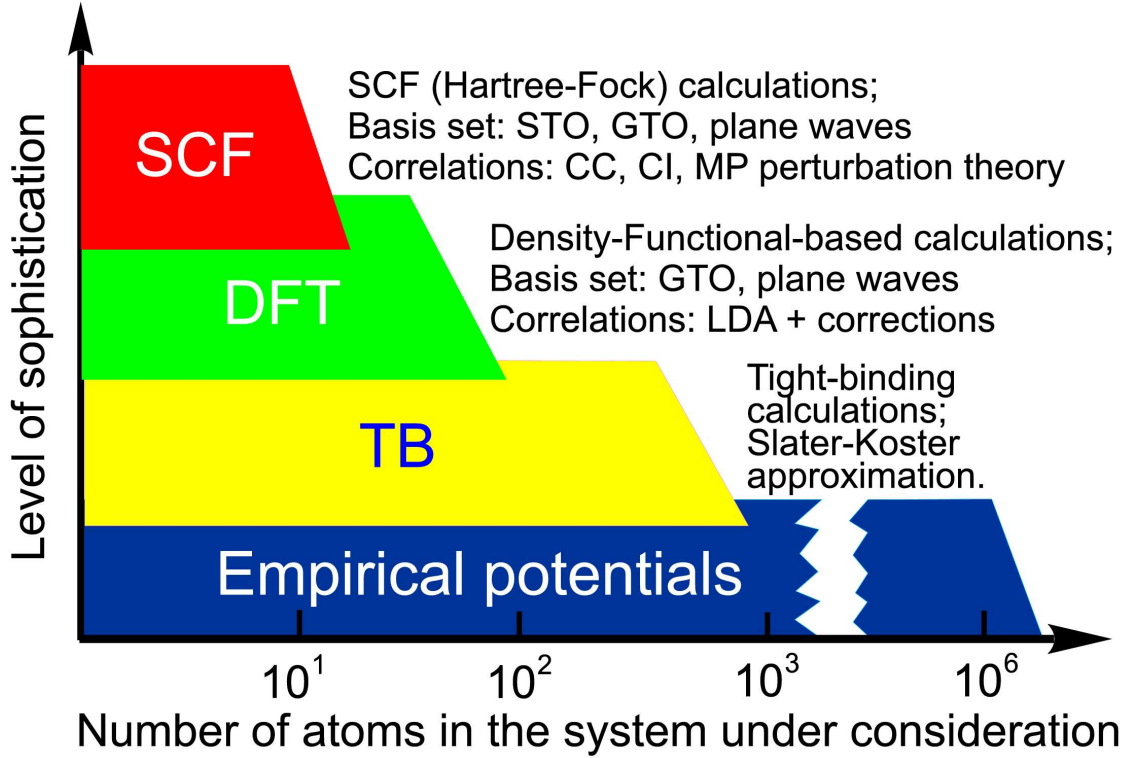[1]H depends on the distribution of electrons

Figure 1: Methods in computational materials science (thankfully taken from [2])

ton operator with a parameterized Hamilton matrix. For this reason, one commonly does not calculate the explicit form of the basis set. "Atomic-like" means that it has the same symmetry properties as the atomic orbitals.

The concept as sketched has been firstly implemented by KOSTER and SLATER [6] in 1954. Concerning the appliance to the material of our primary interest, Silicon, have a look at the paper of CHADI and COHEN [7].

We start with our crystal, firstly choosing the crystallographic axes as the coordinate axes. The *position* of an *atom* in the primitive cell denoted by j decomposes into $\mathbf{r}_{jl} = \mathbf{R}_j + \mathbf{r}_l$, where $\mathbf{R}_j$ denotes the *position* of the j-th *primitive cell* of the Bravais lattice and $\mathbf{r}_l$ is the *position* of the *atom l* within the primitice cell. Let $h(\mathbf{r})$ be the *Hamiltonian* for the *isolated atom l* with its nucleus chosen as the origin. The *Hamiltonian* for the *atom* located at $\mathbf{r}_{jl}$ is given by $h_l(\mathbf{r} - \mathbf{r}_{jl})$. Hence the wave equation for h_l reads

$$h_l \varphi_{ml}(\mathbf{r} - \mathbf{r}_{jl}) = E_{ml} \varphi(\mathbf{r} - \mathbf{r}_{jl})$$

where $E_{ml}...eigenvalues$, $\varphi_{ml}...eigenfunctions$ of the state indexed m.

Next we assume that the *Hamiltonian* for the *crystal* $H(\mathbf{k})$ is equal to the sum of the *atomic Hamiltonians* H_0 and a *Hamiltonian* H_{int} describing the *interaction* between the different atoms. If the latter is weak, we can diagonalize $H(\mathbf{k})$ by pertubation theory. The unperturbed wave functions can be constructed as linear combinations of the atomic wave functions. Additionally we use the translational symmetry of the crystal to express

the wavefunctions as Bloch functions (N ... *number* of primitive unit cells within the crystal)

$$\Phi_{ml}(\mathbf{k}) = \frac{1}{\sqrt{N}} \sum_j e^{i\mathbf{r}_{jl}\mathbf{k}} \varphi_{ml}(\mathbf{r} - \mathbf{r}_{jl}) \tag{2}$$

and the *eigenfunctions* of $H(\mathbf{k})$ are therefore

$$\psi(\mathbf{k}) = \sum_{m,l} C_{ml}\Phi_{ml}(\mathbf{k})$$

Due to our initial position we now have to turn to the minimization of the Rayleigh ratio

$$E(\mathbf{k}) = \frac{\langle\psi| H |\psi\rangle}{\langle\psi|\psi\rangle}$$

with respect to the coefficients C_{ml}. This leads to the generalized eigenvalue problem

$$\sum_{m,l} (H_{ml,m'l'} - E(\mathbf{k})S_{mm'll'})C_{m'l'}(\mathbf{k}) = 0$$

where $H_{ml,m'l'}$ is the *Hamiltonian matrix element* $\langle\Phi_{ml}(\mathbf{k})| H |\Phi_{m'l'}(\mathbf{k})\rangle$ and $S_{mm'll'}$ is the *overlap matrix element* $\langle\Phi_{ml}(\mathbf{k}) | \Phi_{m'l'}(\mathbf{k})\rangle$, both expressed in our basis $\{|\Phi_{ml}(\mathbf{k})\rangle\}$. For simplicity, it is common (at least in textbooks) to set the overlap matrix to the unity matrix $S_{mm'll'} = \delta_{mm'}\delta_{ll'}$. In other words the basis functions of different atoms are considered to be orthogonal to each other. This is, of course, an uncontrolled approximation, and in all modern tight-binding codes, the correct overlap matrix is taken into account. On the other hand, one can actually create an orthogonal set from an unorthogonal one, e.g. by applying the Löwdin scheme[2]. Anyway, with our approximation we get the familiar eigenvalue problem

$$\sum_{m,l} (H_{ml,m'l'} - E(\mathbf{k})\delta_{mm'}\delta_{ll'})C_{ml} = 0 \tag{3}$$

which can be solved by diagonalizing the matrix $(H_{ml,m'l'} - E(\mathbf{k}))$. The solution gives the eigenvalue spectrum (a set of E's), and the corresponding eigenfunctions $\psi(\mathbf{k})$.

2.2 *s*-, *p*-orbitals

Our basis functions are *s*-, and *p*-orbitals. For this reason we now take a closer look at them as they evolve from the H-atom calculation. The total wave function ofor the hydrogen atom reads [8]

$$\psi(r, \theta, \phi) = R_{nl}(r)Y_l^m(\theta, \phi)$$

---

[2]The scheme preserves even the symmetry properties of the original set. But the orthogonalization transformation is valid only for a single configuration of the system (e.g. Si in the diamond structure); if the configuration changes (e.g. liquid Si), a different transformation is required to orthogonalize the atomic-like orbitals. Furthermore, orthogonalized functions have a wider extent than the equivalent non-orthogonal ones. Therefore, if the basis is assumed to consist of orthogonalized functions, the Hamilton matrix should be expected to have interactions between more distant neighbors than it would otherwise have.
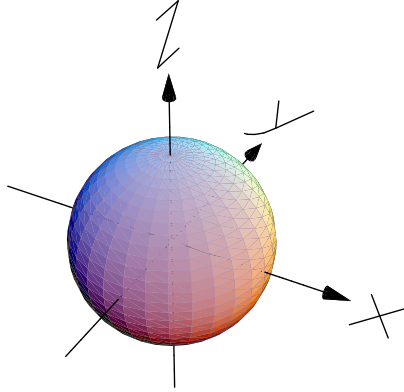
Figure 2: The s-orbital

where $Y_l^m(\theta, \phi)$ is a *spherical harmonic function* and R_{nl} is the *radial solution*. n, l and m are the *principal*, *angular-momentum* and *magnetic quantum numbers*, respectively. For example, the 1s-atomic orbital ($n = 1$ and $l = m = 0$) is spherically symmetric and is taken as positive finite (see Figure 2).

For the p-orbitals ($n = 2, l = 1, m = \pm 1, 0$), we work with the Cartesian representation, such that the three orthogonal p-orbitals are along the x-, y-, z-axes.

The corresponding wave function then reads

$$\psi_{nlm}(x, y, z) = \sqrt{\frac{3}{4\pi}} R_{nl}(r) \begin{cases} x/r \\ y/r \\ z/r \end{cases}$$

where $r = \sqrt{x^2 + y^2 + z^2}$

Another commonly used basis set are sp^n-hybrid orbitals (mixing of the s state with n of the others, on the same atom located, p-orbitals). The reason for considering such hybrids is, that they often allow much greater insight into the band structure and stability of a particular crystal structure.

Well, at the moment we have an eigenvalue problem and a basis set. What do we need next? Right! A cool beer! So lets grab one and then turn to the Hamiltonian and its matrix elements.
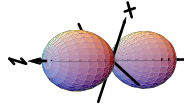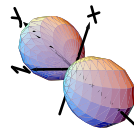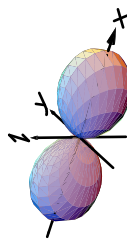
Figure 3: The *p*-orbitals

2.3 Building up H

As already mentioned, our H for the whole crystal is of the form

$$H(\mathbf{k}) = H_0 + H_{int}$$

For Silicon our basis consists of $3s, 3p_x, 3p_y, 3p_z$, centered around each atom. Effects of inner shell electrons can be effectively included using pseudopotential methods.

The first step consists in writing the matrix elements between our basis states in terms of matrix elements between atomic states. In doing so we have to keep in mind, that sums of states with different $\mathbf{k}$ are not valid Bloch states, and therefore we should only have matrix elements between basis states with the same value for $\mathbf{k}$. By substituting (2) into (3) we arrive at

$$
\begin{aligned}
\langle \Phi_{ml}(\mathbf{k})| \, H(\mathbf{k}) \, |\Phi_{m'l'}(\mathbf{k})\rangle &= \frac{1}{N} \sum_{j,j'}^{N} e^{i(\mathbf{r}_{jl} - \mathbf{r}_{j'l'})\mathbf{k}} \langle \phi_{ml}(\mathbf{r} - \mathbf{r}_{jl})| \, H \, |\phi_{m'l'}(\mathbf{r} - \mathbf{r}_{j'l'})\rangle \quad (4) \\
&= \frac{1}{N} \int \sum_{j,j'}^{N} e^{i(\mathbf{r}_{jl} - \mathbf{r}_{j'l'})\mathbf{k}} \varphi_{ml}^*(\mathbf{r} - \mathbf{r}_{jl}) H \varphi_{m'l'}(\mathbf{r} - \mathbf{r}_{j'l'}) d\mathbf{r}
\end{aligned}
$$

The key idea is that we do not calculate these integrals explicitly. Instead of that we approximate them by analytical functions, which depend on atom types, atom separation and orbital mutual orientation. The first approximation down this road is the "two-center approximation", which means that we simplify the Hamiltonian by just considering those potentials centred on the same sites as the atomic states in the matrix element. The effect of the other potentials can be incorporated as a mean field type interaction.

Let's look at first at the diagonal matrix elements. The implementation of our orthogonality assumption yields

$$\langle \Phi_{ml}(\mathbf{k})| \, H(\mathbf{k}) \, |\Phi_{m'l'}(\mathbf{k})\rangle = \frac{1}{N} \sum_{j,j'} e^{i(\mathbf{r}_{jl} - \mathbf{r}_{j'l'})} E_k \delta_{ll'} \delta_{jj'} = \frac{1}{N} \sum_{j,j'} E_k \delta_{ll'} \delta_{jj'} = E_k$$

Hence for the s-orbital we get $E_s = \langle s| \, E \, |s\rangle$ whereas for the p_i-orbitals $\langle p_x| \, H \, |p_x\rangle = \langle p_y| \, H \, |p_y\rangle = \langle p_z| \, H \, |p_z\rangle = E_p$. Both parameters are chosen to fit results of experiments or first-principle simulations.

Now we turn to the off-diagonal elements. For the sake of simplicity we will work out the details from a rather phenomenological point of view. What happens if we bring two Si atoms together? Well, their atomic orbitals will overlap to form a diatomic molecule. The interaction between the two atomic orbitals produces two new atomic orbitals. One of the resultant orbitals is symmetric with respect to the interchange of the two atoms and is known as the "bonding orbital". The other, antisymmetric orbital is called the "antibonding orbital". s-orbitals can obviously overlap in just one way, whereas there are two possibilities for p-orbitals (Figure 4). When they overlap along the direction of the p-orbitals, they are said to form σ-bonds. When they overlap in a direction perpendicular to the p-orbitals they are said to form π-bonds. Additionally we have to
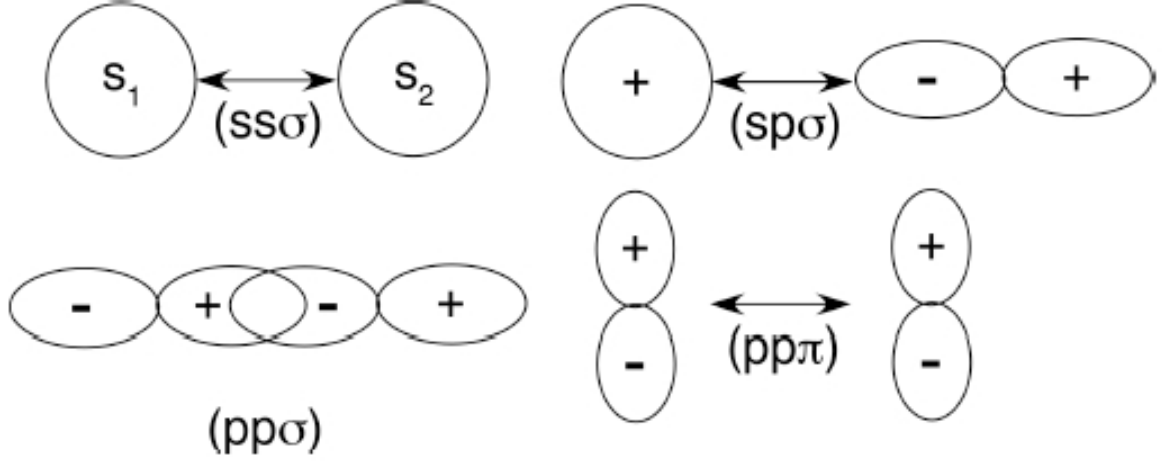
Figure 4: The 4 hopping parameter (thankfully taken from [9]

take the bonding between $s-$ and $p-$orbitals into account. We therefore end up with only four "overlap parameters" or "hopping integrals"

- $(ss\sigma)$: $\langle s_1 | H | s_2 \rangle = V_{ss\sigma} = s(r)V_{ss}$

- $(sp\sigma)$: $\langle s_1 | H | p_{z,2} \rangle = V_{sp\sigma} = s(r)V_{ss\sigma}n$

- $(pp\sigma)$: $\langle p_{z,1} | H | p_{z,2} \rangle = V_{pp\sigma} = s(r)[l^2 V_{pp\sigma} + (1 - l^2)V_{pp\pi}]$

- $(pp\pi)$:

    - $\langle p_{x,1} | H | p_{x,2} \rangle = V_{pp\pi} = s(r)[l^2 V_{pp\sigma} + (1 - l^2)V_{pp\pi}]$
    - $\langle p_{y,1} | H | p_{y,2} \rangle = V_{pp\pi} = s(r)[m^2 V_{pp\sigma} + (1 - m^2)V_{pp\pi}]$

    where $l = cos(\theta_x) = x/r$, $m = cos(\theta_y) = y/r$, $n = cos(\theta_z) = z/r$

The way we have written down these matrix elements foreshadows how we will deal with them further on. As in our case, we will simply take numerical values for $V_{ss\sigma}$, $V_{sp\sigma}$, etc. from [7] and [10], but one can also track them down to a function $s(r)$ (which just depends on the atom separation) multiplied by a parameter [6] (which depends on the atom type) . A general expression for the four overlap parameters $V_{ss\sigma}$, etc. is given by

$$V_{ll'm} = \tau_{ll'm} \frac{\hbar^2}{md^2}$$

where $d...nearest\text{-}neighbor\ distance$, $m...mass$ of the electron, and $\tau_{ll'm}$ is a *factor* depending on the crystal symmetry.

We have now a somewhat schematic picture of our matrix elements. Before we go ahead, let's make a small sidestep. The extension of bonding and antibonding orbitals to crystals works, if we assume, that the orbitals of each crystal overlap with those of its nearest neighbor only. This is a reasonable approximation for most solids. In this
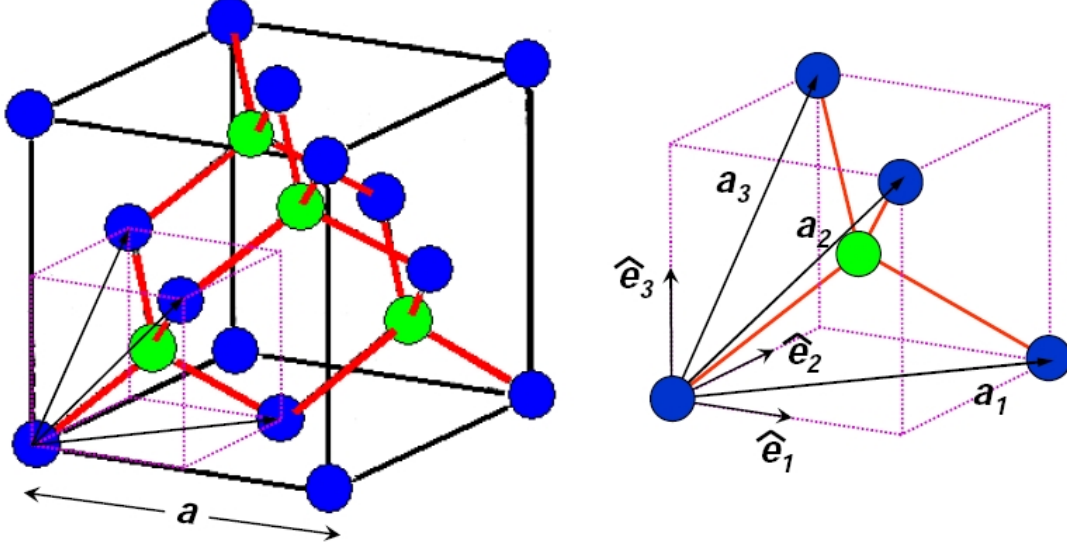
Figure 5: The structure of diamond (thankfully taken from [12])

new physical situation bonding and antibonding orbitals broaden into bands. Those occupied by electrons form valence bands (bonding orbitals) while the empty ones form conduction bands (antibonding orbitals).

We are now ready to apply all our considerations to Silicon. It has a diamond-like crystal structure, which can be thought of as two interpenetrating fcc-Bravis lattices, displaced by the vector $(a/4)[1,1,1]$ (a...*lattice constant*). Have a look at Figure 5. An applet, demonstrating the 3D structure can be found on the website [11]. The unit cell is spanned by the vectors $\mathbf{a} = (a/2)[1,1,0]$, $\mathbf{b} = (a/2)[1,0,1]$, $\mathbf{c} = (a/2)[0,1,1]$ It contains two atoms at $[0,0,0]$ and $(a/4)[1,1,1]$ (i.e. $l = 1,2$). Since we have 4 atomic states at each atom, each unit cell contains 8 basis states. $H(\mathbf{k})$ will be an 8×8-matrix and we will get 8 eigenvalues (with respect to $\mathbf{k}$) and 8 energy bands. The restriction to next-neighbor-interaction means, that the sum in (4) will only run over the atom itself and its four neighbors.

The building up of the matrix is rather time-consuming and for that reason let's stick to the calculation of two matrix elements, namely the transition element $s_2 \to s_1$ and $p_{x,2} \to s_1$. By "1" we think of the atom at the origin and by "2" of the atom at $(a/4)[1,1,1]$. The four neighbors of the atom at $[0,0,0]$ are

$$\mathbf{d}_1 = (a/4)[1,1,1], \mathbf{d}_2 = (a/4)[1,-1,-1], \mathbf{d}_3 = (a/4)[-1,1,-1], \mathbf{d}_4 = (a/4)[-1,1,1]$$

Putting this into (4) we get for the $s_1 \to s_2$ matrix element

$$\langle s_1 | H(\mathbf{k}) | s_2 \rangle = (e^{i\mathbf{k}\mathbf{d}_1} + e^{i\mathbf{k}\mathbf{d}_2} + e^{i\mathbf{k}\mathbf{d}_3} + e^{i\mathbf{k}\mathbf{d}_4}) \underbrace{\langle s_1 | H_{\text{int}} | s_2 \rangle}_{\sim V_{ss\sigma}}$$

In the same manner we can express the other elements in terms of the overlap parameters $V_{ss\sigma}$, $V_{pp\sigma}$ and $V_{pp\pi}$. For example $\langle s_1 | H(\mathbf{k}) | p_{x,2} \rangle$ contains four terms involving the
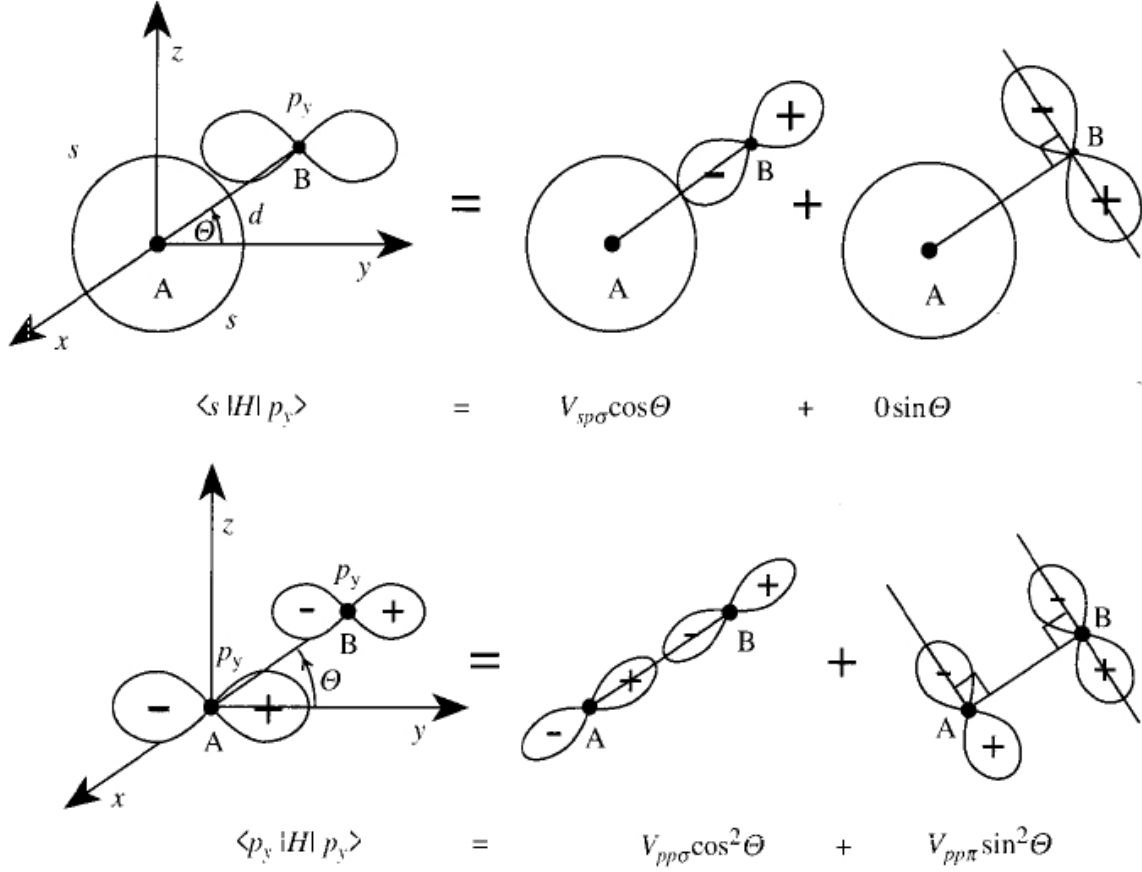
Figure 6: Projection of the overlap parameter between an s- and a p_y-orbital, and between p_y-orbitals, along the vector $\mathbf{d}$ joining the two atoms and perpendicular to $\mathbf{d}$. (thankfully taken from [1])

four phase vectors $exp\{i\mathbf{k}\mathbf{d}_i\}$ and the matrix elements $\langle s_1|\,H_{\text{int}}\,|p_{x,2}\rangle$. However since our coordinate system is fixed to the crystallographic axes $\langle s_1|\,H_{\text{int}}\,|p_{x,2}\rangle$ has to be decomposed into σ and π components for each nearest neighbor (see Figure 6). This introduces a factor $cos\theta = \pm 1/\sqrt{3}$. The $+$ or $-$ sign depends on whether the s-orbital lies in the direction of the positive or negative lobe of the p_x-orbital. As a result, it is convenient to introduce a new set of overlap parameters appropriate for the diamond lattice

$$V_{ss} = 4V_{ss\sigma} \quad , \quad V_{sp} = -\frac{4}{\sqrt{3}}V_{sp\sigma}$$

$$V_{xx} = \frac{4}{3}(V_{pp\sigma} + 2V_{pp\pi}) \quad , \quad V_{xx} = \frac{4}{3}(V_{pp\sigma} - V_{pp\pi})$$

With this notation our example reads $\langle s_1|\,H(\mathbf{k})\,|p_{x,2}\rangle = \langle s_1(\mathbf{r})|\,H_{\text{int}}\,|p_{x,2}(\mathbf{r} - \mathbf{d}_1)\rangle = -V_{sp\sigma}/\sqrt{3} = V_{sp}/4$. The remaining three matrix elements are related by symmetry. For example, a two-fold rotation about the y-axis will transform [x,y,z] into [-x,y,z], hence $\mathbf{d}_1$ is transformed into $\mathbf{d}_3$. The s-symmetry wave function $|s_1\rangle$ is unchanged while the p-

10

symmetry wave function $|p_{x,2}\rangle$ is transformed into -$|p_{x,2}\rangle$ under this rotation. As a result, $\langle s_1(\mathbf{r})|\, H_{\text{int}}\, |p_{x,2}(\mathbf{r}-\mathbf{d}_3)\rangle = -\langle s_1(\mathbf{r})|\, H_{\text{int}}\, |p_{x,2}(\mathbf{r}-\mathbf{d}_1)\rangle$. By applying similar symmetry operations we can show that

$$\sum_i e^{id_i k}\, \langle s_1(\mathbf{r})|\, H_{\text{int}}\, |p_{x,2}(\mathbf{r}-\mathbf{d}_i)\rangle = \frac{1}{4}V_{sp}(e^{i\mathbf{d}_1\mathbf{k}} + e^{i\mathbf{d}_2\mathbf{k}} - e^{i\mathbf{d}_3\mathbf{k}} - e^{i\mathbf{d}_4\mathbf{k}})$$

In the same manner one can build all other elements. But we skip the details and turn straightly to the resulting matrix $\langle \Phi(\mathbf{k})|\, H(\mathbf{k})\, |\Phi(\mathbf{k})\rangle$

$$
\begin{pmatrix}
 & s_1 & s_2 & p_{x,1} & p_{y,1} & p_{z,1} & p_{x,2} & p_{y,2} & p_{z,2} \\
 & \downarrow & \downarrow & \downarrow & \downarrow & \downarrow & \downarrow & \downarrow & \downarrow \\
s_1 \rightarrow & E_s & V_{ss}g_1 & 0 & 0 & 0 & V_{sp}g_2 & V_{sp}g_3 & V_{sp}g_4 \\
s_2 \rightarrow & V_{ss}g_1^* & E_s & -V_{sp}g_2^* & -V_{sp}g_3^* & -V_{sp}g_4^* & 0 & 0 & 0 \\
p_{x,1} \rightarrow & 0 & -V_{sp}g_2 & E_p & 0 & 0 & V_{xx}g_1 & V_{xy}g_4 & V_{xy}g_2 \\
p_{y,1} \rightarrow & 0 & -V_{sp}g_3 & 0 & E_p & 0 & V_{xy}g_4 & V_{xx}g_1 & V_{xy}g_2 \\
p_{z,1} \rightarrow & 0 & -V_{sp}g_4 & 0 & 0 & E_p & V_{xy}g_2 & V_{xy}g_3 & V_{xx}g_1 \\
p_{x,2} \rightarrow & V_{sp}g_2^* & 0 & V_{xx}g_1^* & V_{xy}g_4^* & V_{xy}g_2^* & E_p & 0 & 0 \\
p_{y,2} \rightarrow & V_{sp}g_3^* & 0 & V_{xy}g_4^* & V_{xx}g_1^* & V_{xy}g_3^* & 0 & E_p & 0 \\
p_{z,2} \rightarrow & V_{sp}g_4^* & 0 & V_{xy}g_2^* & V_{xy}g_2^* & V_{xx}g_1^* & 0 & 0 & E_p
\end{pmatrix}
\quad (5)
$$

where

$$g_1 = g_1(\mathbf{k}) = (1/4)[e^{i\mathbf{k}\mathbf{d}_1} + e^{i\mathbf{k}\mathbf{d}_2} + e^{i\mathbf{k}\mathbf{d}_3} + e^{i\mathbf{k}\mathbf{d}_4}]$$
$$g_2 = g_2(\mathbf{k}) = (1/4)[e^{i\mathbf{k}\mathbf{d}_1} + e^{i\mathbf{k}\mathbf{d}_2} - e^{i\mathbf{k}\mathbf{d}_3} - e^{i\mathbf{k}\mathbf{d}_4}]$$
$$g_3 = g_3(\mathbf{k}) = (1/4)[e^{i\mathbf{k}\mathbf{d}_1} - e^{i\mathbf{k}\mathbf{d}_2} + e^{i\mathbf{k}\mathbf{d}_3} - e^{i\mathbf{k}\mathbf{d}_4}]$$
$$g_4 = g_4(\mathbf{k}) = (1/4)[e^{i\mathbf{k}\mathbf{d}_1} - e^{i\mathbf{k}\mathbf{d}_2} - e^{i\mathbf{k}\mathbf{d}_3} - e^{i\mathbf{k}\mathbf{d}_4}]$$

We now have to find the eigenvalues of this matrix (for a given $\mathbf{k}$). This is done best numerically.

2.4 Numerical solution

The Mathematica notebook, I'm referring here to, can be found on the same webpage as this document [13] . The numerical solution of the matrix (5) has been carried out in the section "The calculation of the eigenvalues". You may run the "Intermezzo" initially, because this will enable the measurement of the CPU-time. But what do we need to do exactly?

At first we need numerical values for V_{ss}, V_{xx}, etc. We take them from [7] and [10]. There's the possibility to calculate the band structure of C or Ge as well. Just uncomment the cell with the corresponding values.

Then we define our lattice vectors as a list, as well as the sums (which depend on the vector $\mathbf{k}$). We have to be cautious concerning the definition of the dot product, because this is in Mathematica represented by ".".
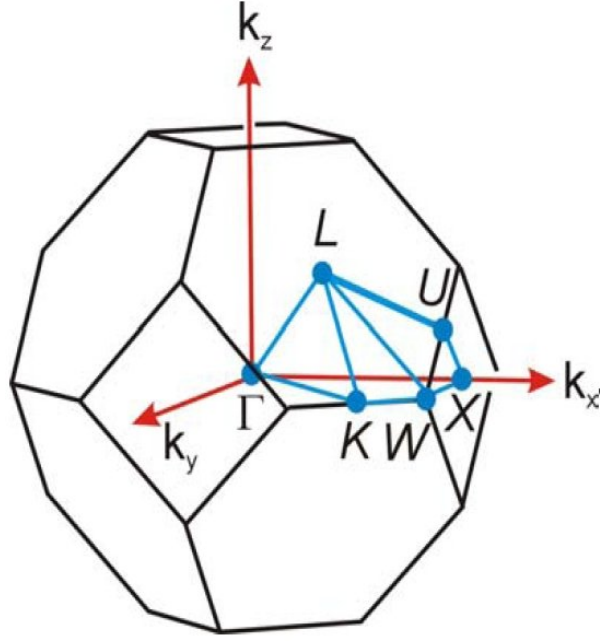
Figure 7: The Brillouin zone for diamond (thankfully taken from [14])

The next step is the definition of the matrix. If we are lucky (hence we have not made any typos), it looks like (5). The function bandenergy[k] calculates the Eigenvalues of the matrix with respect to **k**.

Now we actually start the calculation by generating values for **k** within the first Brillouin zone (Figure [14]), and then calling bandenergy[k]. Whereas the concrete path is to some extense arbitrary, we choose a commonly used one. It runs from $L \Rightarrow \Gamma \Rightarrow X \Rightarrow U == K \Rightarrow \Gamma$. U & K are treated as the same point, which means that they must differ exactly by a reciprocal lattice vector. n is the *number of points*, which are calculated between 0 and 2π. Since not all intervals are equally long, we weight them a little bit. The x values represent the Norm of the **k** vector. Thereby we have to bamboozle a little bit, since the value of k runs back to zero again.

The cell *(∗data manipulation∗)* contains manipulations on the lists, so that we get appropriate sets of (x, y) for our MultipleListPlot. At first we sort the eigenvalues in rising order. Then we transpose them and assign each eigenvalue the corresponding **k** value. Finally we join them all together into the list "bands", which we plot.

3 Results and Outlook

3.1 Discussion

Let's talk breathy about some of the characteristics of the band structure (Figure 8). At points with high symmetry (e.g. Γ) and along directions with high symmetry (e.g. $L \Rightarrow \Gamma$) some of the bands have the same energy and are degenerated respectively.
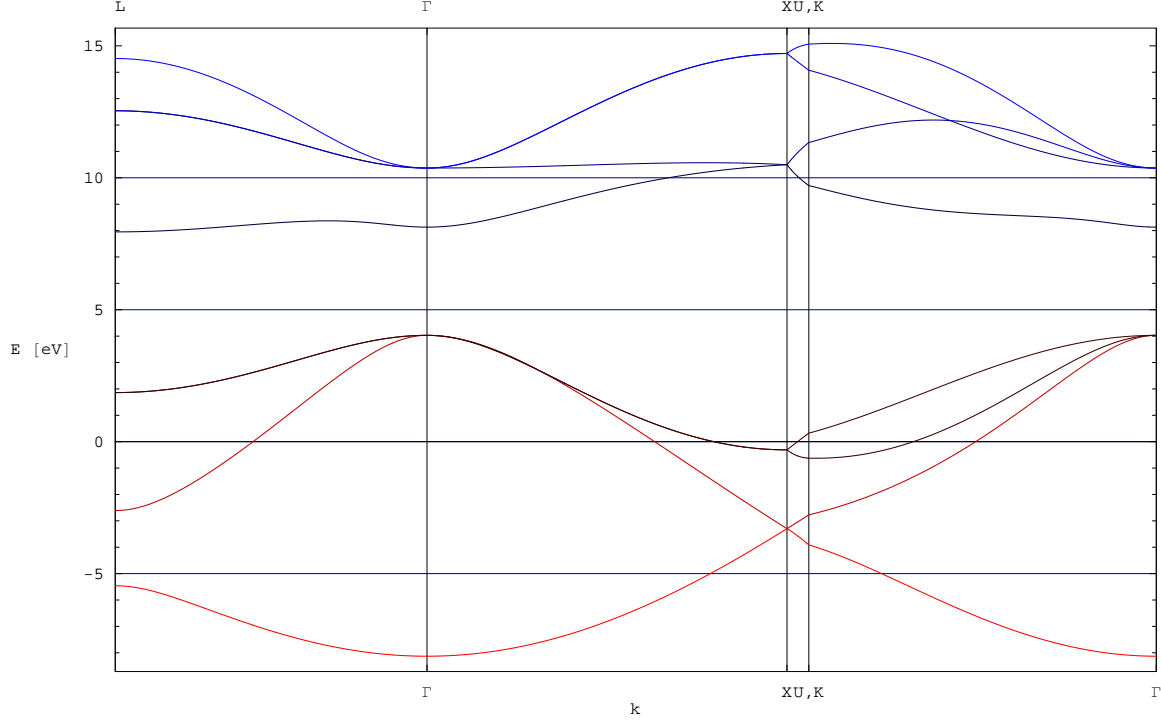
Figure 8: The band structure of Silicon (E in $[eV]$)

Nevertheless we can clearly distinguish between the valence bands and the conduction bands. Concretly, the gap between both has been estimated to be about 3.92 eV. This is far from beautiful if we compare it with its experimental counterpart 1.14 eV. As it turns out, we would have to include second-neighbor interactions to close this discrepancy.

The four lowest bands are totally occupied with the eight electrons of each primitive cell. Hence the conduction bands are empty. But the low gap of 1.14 eV makes excitation possible to some extent. Electrons may get into the codunction bands and Silicon is therefore called a "semiconductor". The electric conductivity raises with increasing temperature, since more and more electron get excited. However, the energy gap is only indirect, since the minimum of the lowest conduction band is not at the same place as the maxima of the highest valence band. This has far-reaching consequences for the optical properties of Silicon.

A comparison with the results of empirical pseudopotential calculations show ([7]), that there's quite a good agreement between both methods for the valence bands. In contrary to the conduction bands, where the electrons are more delocalized and we would have to introduce additional overlap parameters to improve accuracy. However, there is another shortcoming in the tight-binding model presented here. There are only four conduction bands in this model because we have included only four s- and p-orbitals. To correct this problem additional orbitals and overlap parameters are required.

It is also interesting to compare the evolution of s- and p-orbitals into the conduction- and valence bands at the Brillouin zone center for the three group-IV elements Si, Ge,

and gray tin (α-Sn) (see Figure 9). As the lattice constant increases from Si to α-Sn, the overlap parameters $|V_{ss}|$ and $|V_{xx}|$ decreases (the decrease for the latter is greater than for the former). As a result, the ordering of the s- and p-orbitals changes from Si to α-Sn. The Fermi level is located by filling the bands with the eight valence electrons available. In this way it is easily seen that the lowest conduction band at zone center in Si is p-like while the corresponding band in Ge is s-like. In this scheme α-Sn turns out to be a semi-metal because of the lower energies of the bands derived from the s-orbitals.

3.2 Outlook

One of the most interesting extensions is the force calculation. The *force* f_I acting on the ion is

$$f_I = -\frac{dE}{d\mathbf{R}_I} = -d_{\mathbf{R}_I} \langle\psi| H |\psi\rangle$$

ψ_i...eigenstate to H, R_I...position of the ion I

The easiest way to estimate the force is to calculate it numerically by moving the ion into all directions. It can be shown [2] that one has actually just a partial derivative of the energy with respect to the position of the ion ("Hellmann-Feynman"-theorem):

$$f_I = - \langle\psi| \frac{\partial H}{\partial \mathbf{R}_I} |\psi\rangle$$

Forces calculated with the help of this relation are very sensitive to errors in the wave function, which have to be close to exact eigenstates. On the other hand, it saves CPU-time, since one just has to solve the eigenvalue problem once.

Tight binding models have been developed for a variety of materials such as metals, semiconductors, fullerenes and ionic materials. They have been applied to a variety of problems like the calculation of the elastic constants, etc. as well. Just have a look at [4].

In conclusion we have discussed a very powerful and yet simple method to get information about the electronic structure of a material. Due to its semiclassical properties, it represents (and will represent further on) a reliable advance guard for first-principle methods into new undiscovered territory (increasing system size).

References

[1] CARDONA and YU, *Fundamentals of semiconductors*, Springer Verlag, 1996.

[2] KRASHENINNIKOV, Introduction to electronic structure calculations, (http://beam.helsinki.fi/~akrashen/esctmp.html).

[3] ALLAN, ARIAS, JOANNOPOULOS, PAYNE, and TETER, *Rev. Mod. Phys.* **64**, 1045 (1992).

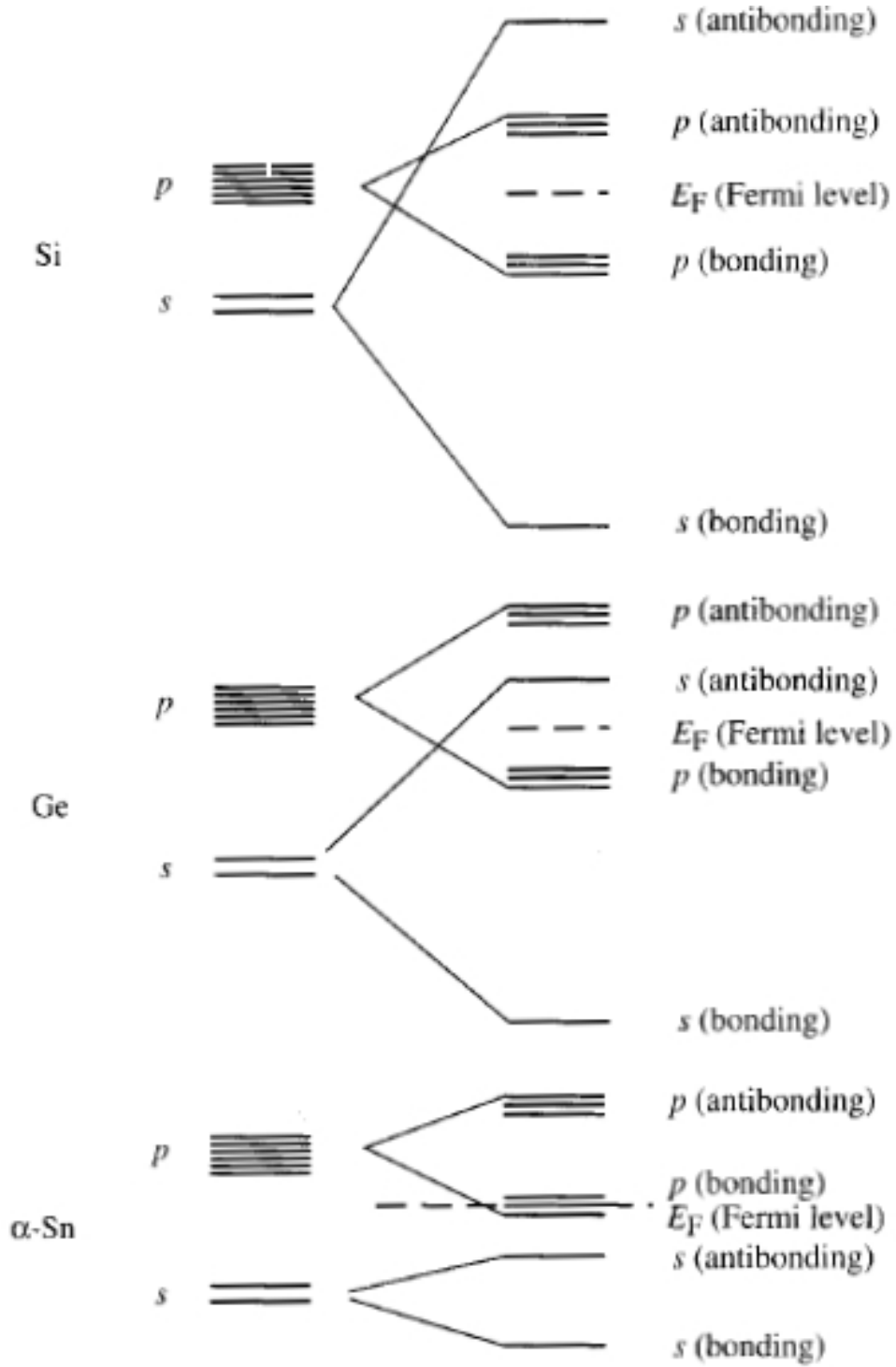[4] BOWLER, GORINGE, and HERNÁNDEZ, *Rep. Prog. Phys.* **60**, 1447 (1997).

Figure 9: Evolution of s- and p-orbitals into the conduction and valence bands at zone center within the tight-binding approximation for Si, Ge and α-Sn. (thankfully taken from [1])

[5] GOEDECKER, *Rev. Mod. Phys.* **71**, 1085 (1999).

[6] KOSTER and SLATER, *Phys. Rev.* **94**, 1498 (1954).

[7] CHADI and COHEN, *Phys. Stat. Sol. (b)* **68**, 405 (1975).

[8] WEISSTEIN, Hydrogen atom,
(http://scienceworld.wolfram.com/physics/HydrogenAtom.html).

[9] NAKANO, PHYS516: Methods of Computational Physics, University of Southern California.

[10] CHADI and QIAN, *Phys. Rev. B* **35**, 1288 (1987).

[11] WIE, Crystal Viewer,
(http://jas2.eng.buffalo.edu/applets/education/solid/unitCell/home.html).

[12] GROSS and EINZEL, Übungen zur Festkörperphysik I und II ,
(http://www.wmi.badw-muenchen.de/E23/lehre/skript/).

[13] PFANNER, The Homepage of Gernot Pfanner,
(http://www-stud.uni-graz.at/~pfannerg/).

[14] BREU, Festkörperchemie II,
(http://www.wmi.badw-muenchen.de/E23/lehre/skript/).